CHAPTER V

PARTIAL OXIDATION OF ISO-OCTANE OVER $Ni/Ce_{0.75}Zr_{0.25}O_2$ AND Ni/β''-Al_2O_3 CATALYSTS

5.1 Abstract

In this study, the partial oxidation of *iso*-octane over $Ni/Ce_{0.75}Zr_{0.25}O_2$ and Ni/β''-Al_2O_3 catalysts was investigated. The results indicated that $Ni/Ce_{0.75}Zr_{0.25}O_2$ is more active than Ni/β''-Al_2O_3. The partial oxidation products were mainly H_2 and CO for $Ni/Ce_{0.75}Zr_{0.25}O_2$ catalyst with hydrogen selectivity up to 53% in the temperature range of 550 - 800°C with a C/O feed ratio of 1. The H_2/CO ratio was in the range of 1.3-1.7 depending on the operating temperature. It was noticed that at temperatures above 700°C, the presence of methane was detected. On the other hand, the main products of *iso*-octane partial oxidation over Ni/β''-Al_2O_3 catalyst were CO_2 and i-C_4H_8 at temperatures below 650°C while H_2 and CO along with small amount of hydrocarbons such as CH_4, C_2H_4, C_2H_6 and C_3H_6 were obtained at temperatures above 650°C yielding a H_2/CO ratio of about 1.3. As a result, the hydrogen selectivity was lower than that of $Ni/Ce_{0.75}Zr_{0.25}O_2$ catalyst. For both catalysts, the carbon dioxide and carbon monoxide selectivities were decreased whilst the hydrogen and hydrocarbon selectivities were increased with increasing C/O feed ratio. The $Ni/Ce_{0.75}Zr_{0.25}O_2$ catalyst can be operated over a wider C/O feed ratio range than the Ni/β''-Al_2O_3 catalyst resulting in less amount of carbon formed. The presence of steam in the feed yielded a larger amount of hydrogen and less amount of coke formation. Since the *iso*-octane conversion of both catalysts remained unchanged after a prolonged reaction time, a decrease in H_2 selectivity for Ni/β''-Al_2O_3 catalyst may be attributed to the phase change of β''-Al_2O_3 in the presence of steam.

5.2 Introduction

There is currently a great interest in fuel cells as potential replacements of conventional combustion engines or as auxiliary power units in automobiles. The most promising fuel cells would seem to be the ones equipped with a proton exchange membrane (PEM) using hydrogen (Avci *et al.*, 2001; Moon *et al.*, 2001). However, the distribution and on-board storage of hydrogen are major hurdles. Therefore, compact and efficient devices to convert liquid transportation fuels to hydrogen are needed, either in the form of on-board reformers or in stationary facilities supplying refueling stations with hydrogen. It is very likely that for the foreseeable future, we will have to rely on the existing gasoline distribution infrastructure as source of hydrogen for fuel cell equipped vehicles. Hydrogen can be produced from natural gas, naphtha, vacuum residue, refinery off-gas, etc. In transportation, methanol, gasoline, or diesel are suitable fuels (Ahmed and Krumpelt, 2001). Some studies have been focused on the conversion of methanol to hydrogen (Peppley *et al.*, 1999) but an effective distribution infrastructure for this fuel is not in place. The generation of hydrogen from the other fuels, including natural gas, liquefied petroleum gases (LPG), gasoline, and diesel represents attractive alternatives.

There are three main methods for producing hydrogen from hydrocarbons, namely steam reforming (SR), partial oxidation (POX), and autothermal reforming (ATR). In this study we focused on POX. The conversion of heavy hydrocarbons, which are major constituents of gasoline and diesel, to hydrogen by partial catalytic oxidation tends to suffer from coke formation. Hence, there has been emphasis on the development of highly active and coke resistant catalysts for POX (Avci *et al.*, 2001).

Nickel-based catalysts are attractive for POX due to their low cost but Ni is deactivated easily by coke formation and/or its sintering. Thanks to the redox properties of mixed oxide CeO_2-ZrO_2, $Ni/Ce_{0.75}Zr_{0.25}O_2$ catalyst showed high catalytic activity and resistance to coke formation in methane partial oxidation (Pengpanich *et al.*, 2004). The use of ion conducting solid electrolytes as a catalyst support is also of interest. It was reported that several ion-conducting solid

electrolytes, namely H^+, Li^+, Na^+, K^+, Au^+, Ag^+ β"-Al_2O_3 act as good supports for oxidation catalysts (Harkness *et al.*, 1996; Agrawal *et al.*, 1999; Guillet *et al.*, 2003). When ions are conducted to the metal surface, the rate of hydrocarbon oxidation is improved. The use of β"-Al_2O_3 in fuel cell applications was found to be advantageous since it yields higher value chemicals and electricity simultaneously (Kiwi *et al.*, 1991).

In this study, we investigate the activity, selectivity, and stability of both the 5 wt% Ni/$Ce_{0.75}Zr_{0.25}O_2$ and 5 wt% Ni/β"-Al_2O_3 catalysts for *iso*-octane POX in the temperature range of 400-800°C at atmospheric pressure.

5.3 Experimental

5.3.1 Catalyst Preparation

5 wt% Ni/$Ce_{0.75}Zr_{0.25}O_2$ and 5 wt% Ni/β"-Al_2O_3 catalysts were prepared by a conventional impregnation method with nickel salt solutions. The β"-alumina (with Na^+ ion conductor) used as support was supplied from Ionotec (England) while $Ce_{0.75}Zr_{0.25}O_2$ support was prepared by urea hydrolysis followed by the method reported elsewhere (Pengpanich *et al.*, 2002). Each catalyst was thermally treated in air at 500°C for 4 h.

5.3.2 Catalyst Characterizations

The surface areas of the samples were determined by the BET method using a Quantachrome Corporation Autosorb instrument. The samples were outgassed at 250°C for 4 h prior to analysis.

The degree of nickel dispersion was determined by H_2 pulse chemisorption (Quantachrome modeled ChemBET- 3000 TPR/TPD). About 100 mg of sample was placed in a quartz reactor. Prior to pulse chemisorption, the sample was reduced in H_2 atmosphere at 500°C for 1 h. Then the sample was purged with N_2 at 500°C for 30 min and cooled to 50°C in flowing of N_2. A H_2 pulse (pure H_2, 100 μl) was injected into the sample at 50°C. The metal dispersion was calculated by

assuming the adsorption stoichiometry of one hydrogen atom per nickel surface atom.

Temperature programmed reduction (TPR) measurements were carried out to investigate the redox properties over the resultant materials. H_2 was used as a reducing gas. H_2-TPR was carried out in a TPR analyzer (Quantachrome modeled ChemBET- 3000 TPR/TPD) using 50 mg of sample. The sample was pretreated in flowing N_2 (20 ml/min) at 250°C for 30 min prior to running the TPR experiment, and then cooled down to room temperature in N_2. Then, the sample was exposed to a 5% H_2 in N_2 gas mixture at a flow rate of 75 ml/min, and the sample temperature was raised at a constant rate of 10°C/min from room temperature to 950°C. The amount of H_2 consumption during the increasing temperature period was determined by using a TCD signal.

An X-ray diffractometer (XRD) system (Rigaku) equipped with a RINT 2000 wide-angle goniometer using CuK_α radiation and a power of 40 kV x 30 mA was used for examination of the crystalline structure. The intensity data were collected at 25 °C over a 2θ range of 10-90° with a scan speed of 5° (2θ)/min and a scan step of 0.02° (2θ).

Temperature programmed oxidation (TPO) carried out in a TPO reactor analyzer coupled with an FID was used to quantify the amount of coke formation in the spent catalysts. Typically, about 40 mg of sample was heated with a constant rate of 10°C/min from room temperature to 900°C using 2%O_2 in He as an oxidizing gas at a flow rate of 40 ml/min. The output gas was passed to a methanizer packed with 15 wt% Ni/Al_2O_3 as a catalyst prior to the FID detector. After the temperature reached 900°C, 100 µl of CO_2 pulses was injected in order to evaluate the quantity of coke formed.

5.3.3 Catalytic Activity Tests

A fixed-bed quartz tube microreactor (i.d. ∅ 6 mm) was used for conducting the catalytic activity tests for *iso*-octane partial oxidation. Typically, ca. 10 mg of catalyst sample diluted in 90 mg of α-Al_2O_3 was packed between layers of quartz wool. The reactor was placed in an electric furnace equipped with K-type

thermocouples. The catalyst bed temperature was monitored and controlled by Shinko temperature controllers. *iso*-Octane was vaporized from a saturator at 10°C using He as carrier gas. The concentration of *iso*-octane was maintained at 0.8% by mole. Typically, the feed composition was altered to obtain C/O ratios in the range between 0.6 and 1.6, balanced with He. The total flow rate of feed gases was kept at 150 ml/min (GHSV = 80,000 h^{-1}) using Aalborg mass flow controllers. Measurements were carried out at furnace temperatures adjusted sequentially to 400 - 800°C. The product gases were chromatographically analyzed using a Shimadzu GC 14A equipped with a CTR I (Alltech) column for a TCD detector and Porapak® Q (Alltech) column for an FID detector. The conversions (X) were determined by dividing the mole of reactant consumed by the mole of initial reactant. The selectivities (S) reported in this work were calculated by the ratio of the moles of a specific product to the total moles of all products based on dry basis. This definition allows selectivities of each material to sum to unity.

The effect of water on the POX was carried out in a similar system of POX as mentioned above. However, a feed gas mixture composed of 0.8% iso-octane, 3.2% O_2, 2.4% H_2O and balanced with He was used. The total flow rate of feed gases was kept at GHSV = 80,000 h^{-1}. The catalytic activity tests were measured in the temperature range of 400 – 800°C.

5.4 Results and Discussion

5.4.1 BET Surface Area, Ni Metal Dispersion and H_2-TPR

The BET surface areas, and Ni metal dispersion of the catalysts are shown in Table 5.1. The surface area of Ni/$Ce_{0.75}Zr_{0.25}O_2$ catalyst is significantly higher than that of Ni/β"-Al_2O_3 catalyst. The Ni metal dispersion of Ni/$Ce_{0.75}Zr_{0.25}O_2$ catalyst is also significantly higher than that of Ni/β"-Al_2O_3 catalyst.

Table 5.1 BET surface areas and Ni metal dispersions of the Ni supported catalysts calcined at 500°C

Catalyst	BET surface area (m^2/g)	Ni metal dispersion (%)
5 wt% Ni/β"-Al_2O_3	5.5	1.0
5 wt% Ni/$Ce_{0.75}Zr_{0.25}O_2$	112.0	6.4

H_2- TPR profiles of the catalysts and their supports are shown in Figure 5.1. Based on the TPR profiles, β"-Al_2O_3 does not appear to be reduced significantly while the $Ce_{0.75}Zr_{0.25}O_2$ support shows two reduction peaks at temperatures of about 550 °C and 800°C. It is generally accepted that the first peak is due to the reduction of surface oxygen and the other is the reduction of bulk oxygen. For 5 wt% Ni/$Ce_{0.75}Zr_{0.25}O_2$ sample, the TPR profile shows two peaks located at temperatures of 300 and 370°C and another broad peak at temperatures over 800°C. The first two peaks indicate the reduction of NiO to Ni^0, and the third peak is attributed to the reduction of the support (Montoya *et al.*, 2000). Generally, for supported Ni catalysts the low temperature peak is attributed to the reduction of relatively free NiO particles, while the higher temperature peak corresponds to the reduction of complex nickel oxide species interacting with the support (Roh *et al.*, 2002).

For Ni/β"-Al_2O_3 catalyst, only one reduction peak with the maximum temperature at ca. 530°C was observed. The reduction temperature of Ni/β"-Al_2O_3 is higher than that of Ni/$Ce_{0.75}Zr_{0.25}O_2$. This result indicates that Ni/$Ce_{0.75}Zr_{0.25}O_2$ is easier to reduce than Ni/β"-Al_2O_3 catalyst.

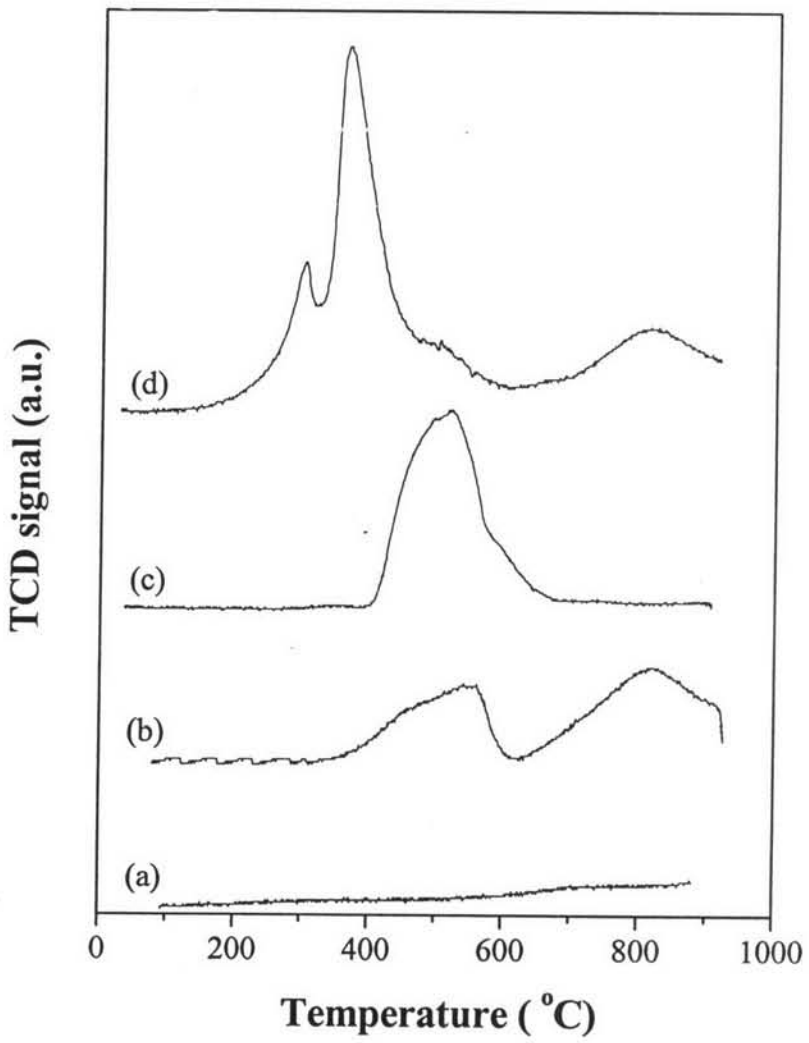

Figure 5.1 H_2-TPR profiles of catalysts calcined at 500°C with heating rate of 10°C/min, a reducing gas containing 5%H_2 in nitrogen with a flow rate of 75 ml/min: (a) β"-Al_2O_3 (b) $Ce_{0.75}Zr_{0.25}O_2$ (c) 5 wt% Ni/β"-Al_2O_3 (d) 5 wt% Ni/$Ce_{0.75}Zr_{0.25}O_2$.

5.4.2 Catalytic Activity for Partial Oxidation of *iso*-Octane

POX of *iso*-octane was carried out over the 5 wt% Ni/β"-Al_2O_3 and Ni/$Ce_{0.75}Zr_{0.25}O_2$ catalysts under the following conditions: space velocity = 80,000 h^{-1} and C/O feed molar ratio = 1. The conversion of *iso*-octane, oxygen consumption and the product selectivities of *iso*-octane POX over Ni/β"-Al_2O_3 and Ni/$Ce_{0.75}Zr_{0.25}O_2$ catalysts are shown in Figures 5.2 and 5.3, respectively. For Ni/β"-Al_2O_3 catalyst, the *iso*-octane conversion started to increase rapidly as temperature increased from 600 to 700°C whereas the Ni/$Ce_{0.75}Zr_{0.25}O_2$ catalyst gave almost 100 % conversion at lower temperatures (ca. 550°C), indicating that Ni/$Ce_{0.75}Zr_{0.25}O_2$ catalyst has higher catalytic activity than Ni/β"-Al_2O_3 catalyst. This may be due to the fact that the Ni/$Ce_{0.75}Zr_{0.25}O_2$ catalyst has much higher BET surface area and a higher degree of Ni metal dispersion, which are essential for the partial oxidation reaction, than the Ni/β"-Al_2O_3 catalyst, as presented in Table 1.

For 5 wt% Ni/β"-Al_2O_3 catalyst (see Figure 5.2), CO_2 and *iso*-butene (i-C_4H_8) were the dominant products at temperature range of 500 to 650°C. It is believed that CO_2 is produced from total oxidation while i-C_4H_8 is produced from cracking reactions at temperatures < 650°C. It was evidient that heavy hydrocarbons could be fragmented by thermal cracking or thermal pyrolysis to lighter hydrocarbons with a high temperature media (Savage, 2000). The cracking temperature can be varied depending on the molecular weight of hydrocarbons. For example, the pyrolysis of alkyl-aromatics occurs at moderate temperatures around 400°C, while pyrolysis of n-heptane and methylcyclohexane can be obtained at temperatures from 680 to 800°C. Hence, we investigated the cracking reaction of *iso*-octane over Ni/β"-Al_2O_3 catalyst and over pure quartz wool (as a blank run) with 0.8% *iso*-octane in He at GHSV of 80,000 h^{-1}. The results are shown in Figures 5.4 and 5.5. The thermal cracking reaction of *iso*-octane started at temperatures above 650°C while the catalytic cracking of *iso*-octane over the catalyst started at lower temperature (above 500°C), with i-C_4H_8 as a dominant product. This suggests that i-C_4H_8 is produced from both thermal and catalytic cracking reactions.

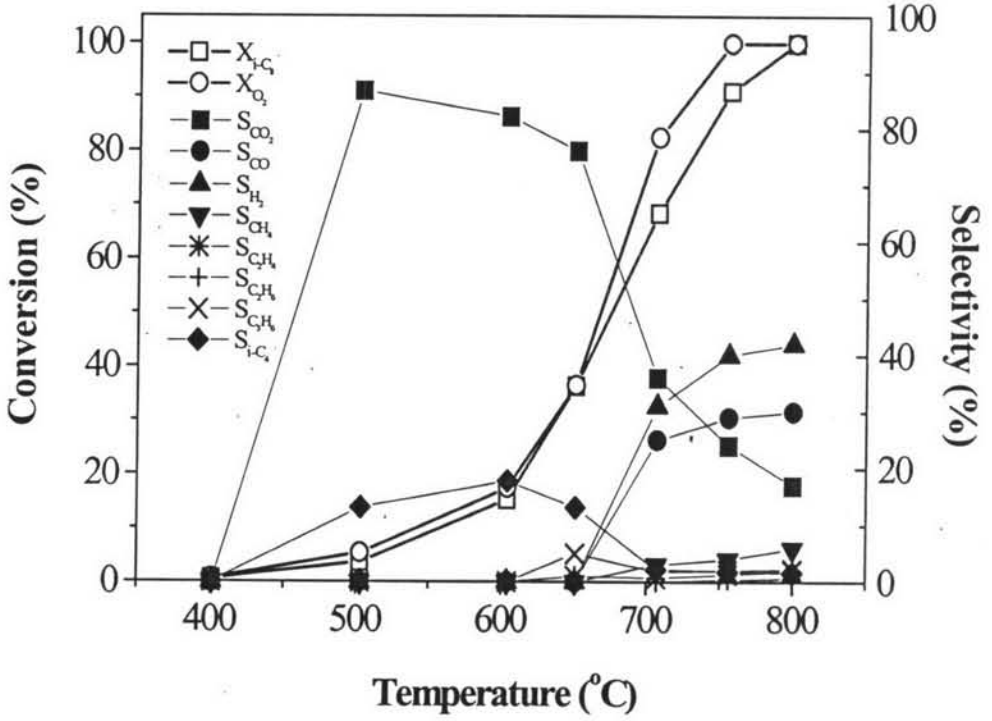

Figure 5.2 *iso*-Octane conversion, oxygen consumption (hollow symbols) and product selectivities (solid symbols) at different temperature for partial oxidation reaction over 5 wt% Ni/β"-Al_2O_3 catalyst at the conditions of space velocity = 80,000 h^{-1} and C/O feed molar ratio = 1.

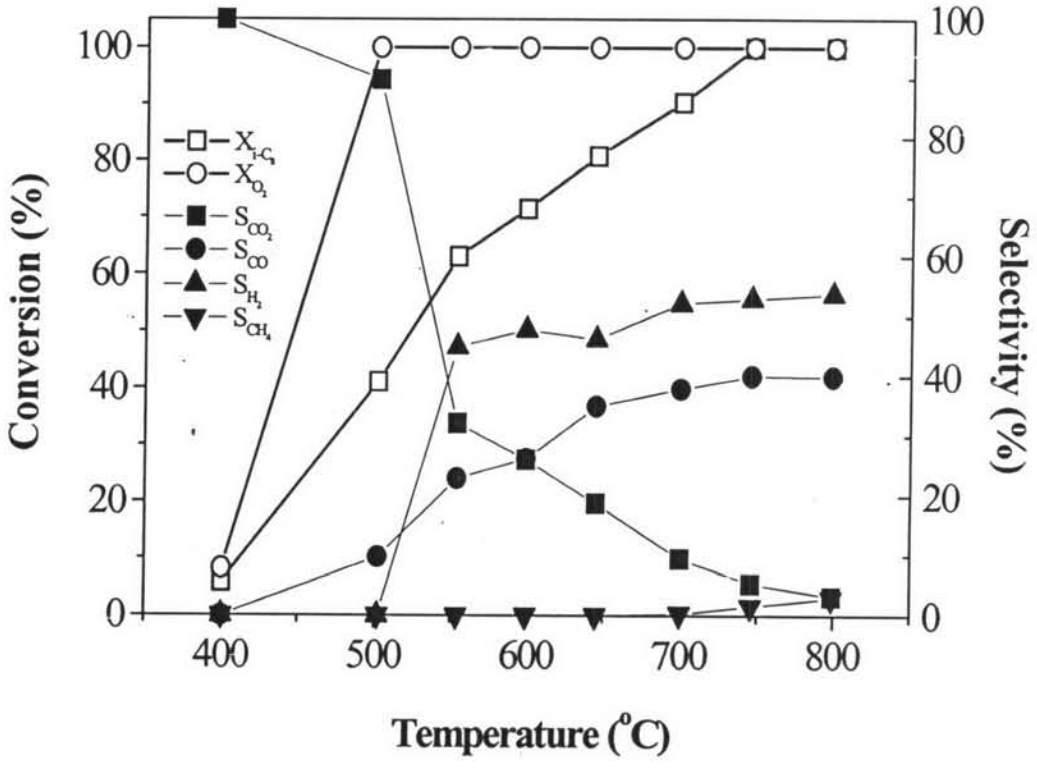

Figure 5.3 *iso*-Octane conversion, oxygen consumption (hollow symbols) and product selectivities (solid symbols) at different temperature for partial oxidation reaction over 5 wt% $Ni/Ce_{0.75}Zr_{0.25}O_2$. catalyst at the conditions of space velocity = 80,000 h^{-1} and C/O feed molar ratio = 1.

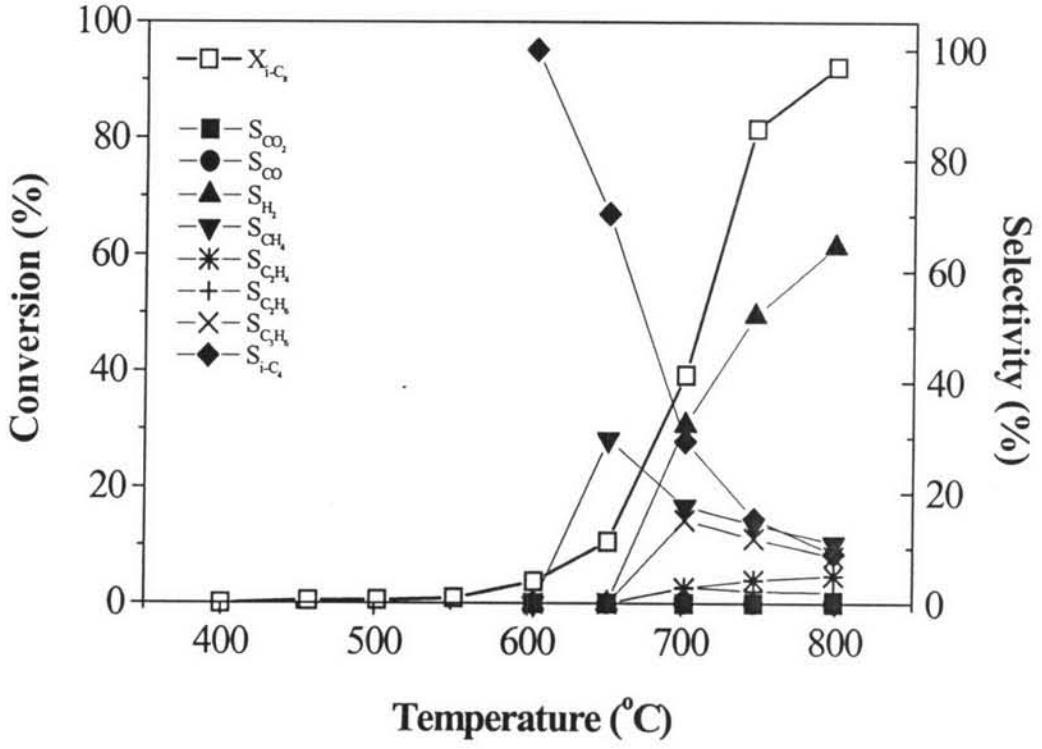

Figure 5.4 *iso*-Octane conversion (hollow symbols) and product selectivities (solid symbols) at different temperature for partial oxidation reaction over a blank run at the conditions of space velocity = 80,000 h^{-1} and *iso*-octane concentration = 1% balanced He.

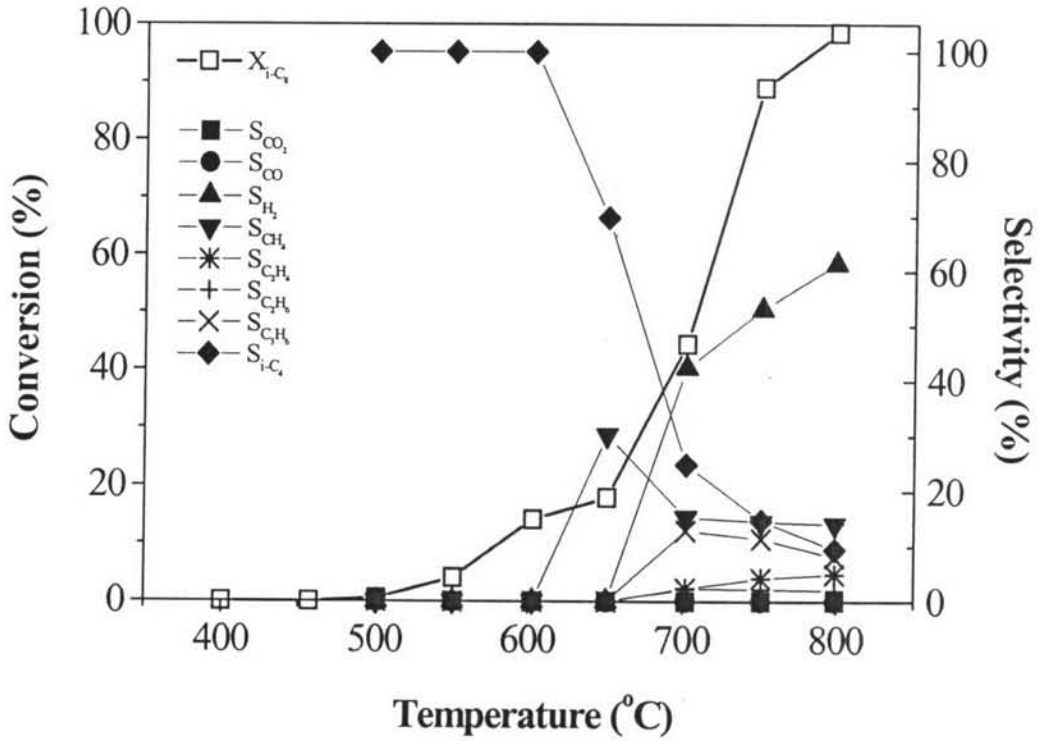

Figure 5.5 *iso*-Octane conversion (hollow symbols) and product selectivities (solid symbols) at different temperature for partial oxidation reaction over 5 wt% Ni/β"-Al_2O_3 catalyst at the conditions of space velocity = 80,000 h^{-1} and *iso*-octane concentration = 1% balanced He.

Above 650°C, the CO_2 and i-C_4H_8 selectivities were decreased whilst other products including CO, H_2, CH_4, C_2H_4, C_2H_6 and C_3H_6 were observed. Under such conditions, the oxygen was completely consumed and a H_2/CO molar ratio of ca. 1.3 was obtained. The light hydrocarbons produced by cracking reactions are then further reformed by either H_2O or CO_2 to yield CO and H_2 products (Pacheco *et al.*, 2003). The olefinic products, C_3H_6 and i-C_4H_8, observed for *iso*-octane partial oxidation over Ni/β"-Al_2O_3 catalyst, might be formed due to β-elimination. This finding is confirmed by results reported by Schmidt and co-workers (Huff *et al.*, 1995; O'Connor *et al.*, 2000). i-C_4H_8 resulted from abstraction of the tertiary hydrogen followed by β-scission of the parent molecule into isobutylene and isobutyl radical. The isobutyl radical can undergo either abstraction of a primary H atom leading to another isobutylene molecule (O'Connor *et al.*, 2000), or β-methyl elimination to form propylene (Huff *et al.*, 1995). The C_2H_4 and C_2H_6 products formed over Ni/β"-Al_2O_3 catalyst at temperatures above 700°C may be due to oxidative coupling of methane. From our earlier results for methane partial oxidation (as shown in Figure 5.6), not only CO_2, CO and H_2 products, but also C_2H_4 and C_2H_6 products were observed for such a catalyst. This suggests that oxidative coupling of methane over Ni/β"-Al_2O_3 may occur. A similar finding was observed by Kiwi *et al.* (1991) who reported that Ni/β"-Al_2O_3 is capable of producing CH_3 radical precursors to generate C_2H_4 and C_2H_6 products. Therefore, the presence of C_2 products observed in the *iso*-octane POX might stem from this reaction.

For 5 wt% Ni/$Ce_{0.75}Zr_{0.25}O_2$ catalyst (see Figure 5.3), at temperatures below 550°C, only CO_2 was observed as product while CO and H_2 became the dominant products at temperatures above 550°C. No C_2 – C_4 products were found over this catalyst. This might be due to the fact that $Ce_{0.75}Zr_{0.25}O_2$ has high reducibility and surface oxygen mobility allowing it to exhibit the high activity for hydrocarbon oxidation reaction (Pengpanich *et al.*, 2004). After the complete consumption of O_2, CO and H_2 started reaching significant levels in the product stream. This infers that the CO and H_2 were produced by reforming rather than by partial oxidation (Praharso *et al.*, 2003). The H_2/CO ratio was in the range of 1.3-2.0 depending on the operating temperature. It was found that the H_2/CO ratio decreased

with increasing operating temperature. From stoichiometry, the H_2/CO ratio from steam reforming is about 2.1 while that for dry reforming is about 0.6. It is apparent that the dry reforming dominates at higher temperatures. The small amount of CH_4 present in the product stream at temperatures above 700°C is believed to be due to the methanation reaction (Ming *et al.*, 2002; Krummenacher *et al.*, 2003).

5.4.3 Catalyst stability

5.4.3.1 The effect of C/O ratio

The C/O feed ratio was varied from 0.6 to 1.6 at a GHSV of 80,000 h^{-1} and the reaction temperature of 700 - 800°C. Table 5.2 shows the effect of C/O feed ratio on the *iso*-octane conversion, oxygen consumption, and product selectivities over 5 wt% Ni/$Ce_{0.75}Zr_{0.25}O_2$ and 5 wt% Ni/β"-Al_2O_3 catalysts at temperatures of 700, 750, and 800°C. For 5 wt% Ni/β"-Al_2O_3 catalyst, it was found that at a given temperature CO and CO_2 selectivities were slightly decreased with increasing C/O feed ratio while the selectivity to H_2 and higher hydrocarbons (C_2's, C_3's, i-C_4H_8) was increased. It might be speculated that with an increasing C/O feed ratio, adsorbed alkane and/or surface carbon concentration on the catalyst surface should increase, further inhibiting O_2 adsorption. Thus, the cracking reaction becomes a dominant reaction (Dietz *et al.*, 1996). For 5 wt% Ni/$Ce_{0.75}Zr_{0.25}O_2$ catalyst, it was found that only CO_2, CO, H_2 and CH_4 products were observed but higher hydrocarbons (C_2's, C_3's) were not observed at all C/O feed ratios. At C/O feed ratios beyond unity, CO and CO_2 selectivities were decreased at a given temperature whereas H_2 and CH_4 selectivities were increased. It is well known that ceria promotes the water gas shift reaction. The decreases in CO and CO_2 selectivties might be due to the onset of water gas shift and methanation with increasing C/O feed ratios.

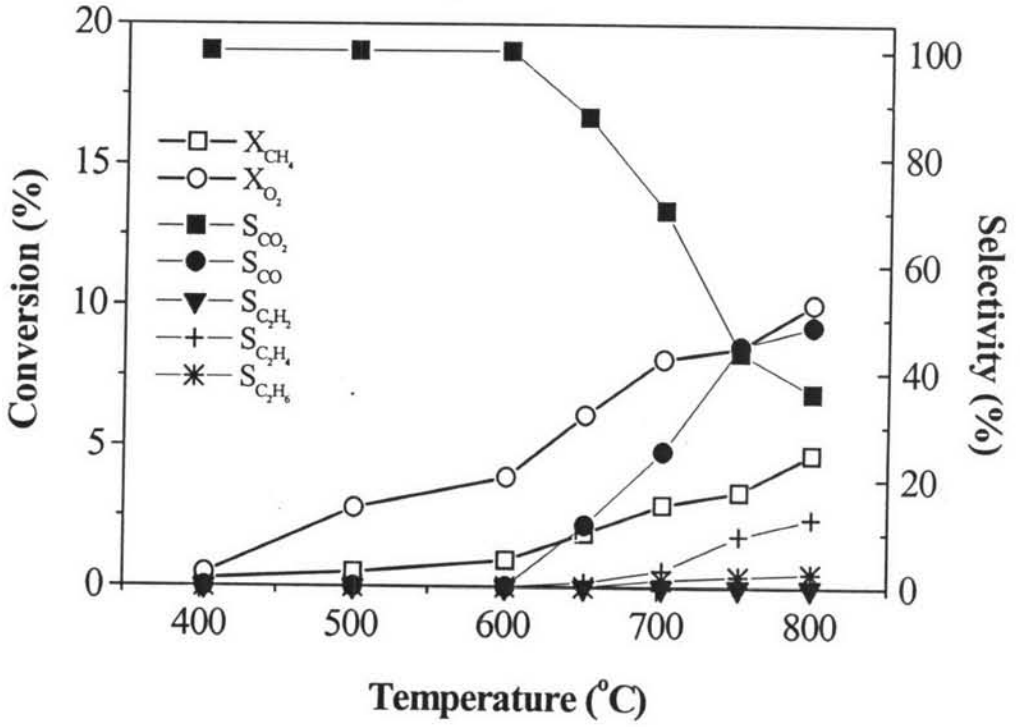

Figure 5.6 CH_4 conversion and product selectivities at different temperature for methane partial oxidation reaction over 5 wt% Ni/β"-Al_2O_3 catalyst at the conditions of space velocity = 80,000 h^{-1} and C/O ratio = 1.

Table 5.2 *iso*-Octane partial oxidation over 5 wt%Ni/$Ce_{0.75}Zr_{0.25}O_2$ and Ni/β"-Al_2O_3 catalysts using various C/O feed ratios

Temperature (°C)	C/O Feed ratio	Ni/$Ce_{0.75}Zr_{0.25}O_2$						
		$X_{i\text{-}C8}$ (%)	X_{O2} (%)	S_{CO2} (%)	S_{CO} (%)	S_{H2} (%)	S_{CH4} (%)	H_2/CO
700	0.6	100	100	25.2	26.1	48.7	0	1.7
750	0.6	100	100	22.6	28.1	49.1	0.2	1.7
800	0.6	100	100	20.4	29.0	49.6	0.9	1.7
700	0.8	94	100	15.5	35.4	48.6	0.3	1.4
750	0.8	100	100	14.4	36.8	47.3	1.2	1.3
800	0.8	100	100	13.2	36.1	49.2	1.4	1.4
700	1.0	90	100	9.4	37.9	52.2	0.3	1.4
750	1.0	100	100	5.3	40.1	52.9	1.6	1.3
800	1.0	100	100	3.2	39.9	53.8	2.9	1.3
700	1.3	85	100	5.9	38.1	55.1	0.5	1.4
750	1.3	94	100	2.7	36.2	57.7	1.8	1.4
800	1.3	100	100	1.9	34.9	55.8	4.4	1.6
700	1.6	75	100	5.4	39.6	53.9	0.7	1.4
750	1.6	87	100	2.4	37.2	56.2	2.7	1.5
800	1.6	100	100	1.7	34.1	56.1	5.1	1.6

Table 5.2 (continued) *iso*-Octane partial oxidation over 5 wt%Ni/$Ce_{0.75}Zr_{0.25}O_2$ and Ni/β"-Al_2O_3 catalysts using various C/O feed ratios

Temperature (°C)	C/O Feed ratio	Ni/β"-Al_2O_3										
		$X_{i\text{-}C8}$ (%)	X_{O2} (%)	S_{CO2} (%)	S_{CO} (%)	S_{H2} (%)	S_{CH4} (%)	S_{C2H4} (%)	S_{C2H6} (%)	S_{C3H6} (%)	S_{iC4} (%)	H_2/CO
700	0.6	70	43	31.7	23.4	29.5	4.2	1.2	0	4.4	5.7	1.3
750	0.6	95	69	22.1	26.5	38.1	5.7	1.3	0.5	3.2	2.5	1.4
800	0.6	100	94	17.0	31.4	40.9	5.7	1.3	0.4	2.0	1.2	1.3
700	0.8	69	45	29.5	24.4	31.7	3.9	1.1	0	4.1	5.3	1.3
750	0.8	94	73	17.5	28.1	43.9	4.5	1.0	0.4	2.6	2.0	1.4
800	0.8	100	94	12.8	32.2	46.9	4.3	1.0	0.3	1.5	1.0	1.5
700	1.0	68	80	35.8	24.7	31.5	3.4	0.7	0	1.8	2.0	1.3
750	1.0	92	100	23.3	25.8	41.7	3.9	1.3	0.4	2.0	1.7	1.6
800	1.0	100	100	16.7	27.7	43.5	5.9	1.9	0.6	2.2	1.5	1.6
700	1.3	58	85	22.8	24.8	34.6	4.3	1.0	0	4.4	7.9	1.4
750	1.3	88	100	15.6	27.2	44.0	4.9	1.4	0.6	3.1	3.2	1.6
800	1.3	100	100	11.8	27.1	45.2	7.0	2.2	0.8	3.2	2.6	1.7
700	1.6	57	87	29.3	19.1	32.2	5.1	1.4	0	5.1	7.8	1.7
750	1.6	85	100	19.4	18.5	44.5	6.0	2.4	0.8	4.1	4.3	2.4
800	1.6	100	100	12.5	20.2	48.2	7.7	2.6	1.0	4.1	3.6	2.4

The coke formation over the spent catalysts was investigated after 6 h-time on stream at 800°C and C/O feed ratios of 0.6, 1.0 and 1.6. The TPO profiles of the catalysts are shown in Figure 5.7. The TPO profiles of 5 wt% $Ni/Ce_{0.75}Zr_{0.25}O_2$ catalyst show a peak centered at ca. 620°C. The peak area was increased with increasing C/O feed ratio. For 5 wt% Ni/β"-Al_2O_3, a very small peak was observed for the catalysts operated at C/O feed ratios ≤ 1.0, while a peak centered at ca. 650°C was observed for the catalysts operated at C/O feed ratio of 1.6. The amounts of carbon deposited on the catalysts are presented in Table 5.3. As the C/O feed ratios ≤ 1.0, the Ni/β"-Al_2O_3 catalyst yielded lower amounts of carbon formed than the $Ni/Ce_{0.75}Zr_{0.25}O_2$ catalyst. However, the amount of carbon deposition over the Ni/β"-Al_2O_3 catalyst was increased by more than two fold as the C/O ratio was higher than unity. This in turn indicates that the $Ni/Ce_{0.75}Zr_{0.25}O_2$ catalyst is more stable under rich conditions than the Ni/β"-Al_2O_3 catalyst due to its good redox properties.

Table 5.3 Amounts of carbon deposited on the catalysts, as determined by TPO, using 2%O_2 in He and heating rate of 10°C/min, after 6 h time on stream at 800°C and C/O ratios of 0.6, 1.0 and 1.6

Catalyst	C/O ratio	*iso*-Octane conversion[a] (%)	Carbon deposits (wt%)
5%Ni/β"-Al_2O_3	0.6	100	0.13
	1.0	100	0.19
	1.6	100	3.88
5%$Ni/Ce_{0.75}Zr_{0.25}O_2$	0.6	100	0.23
	1.0	100	0.85
	1.6	100	1.30

[a] conversion at the end of time on stream (6 h)

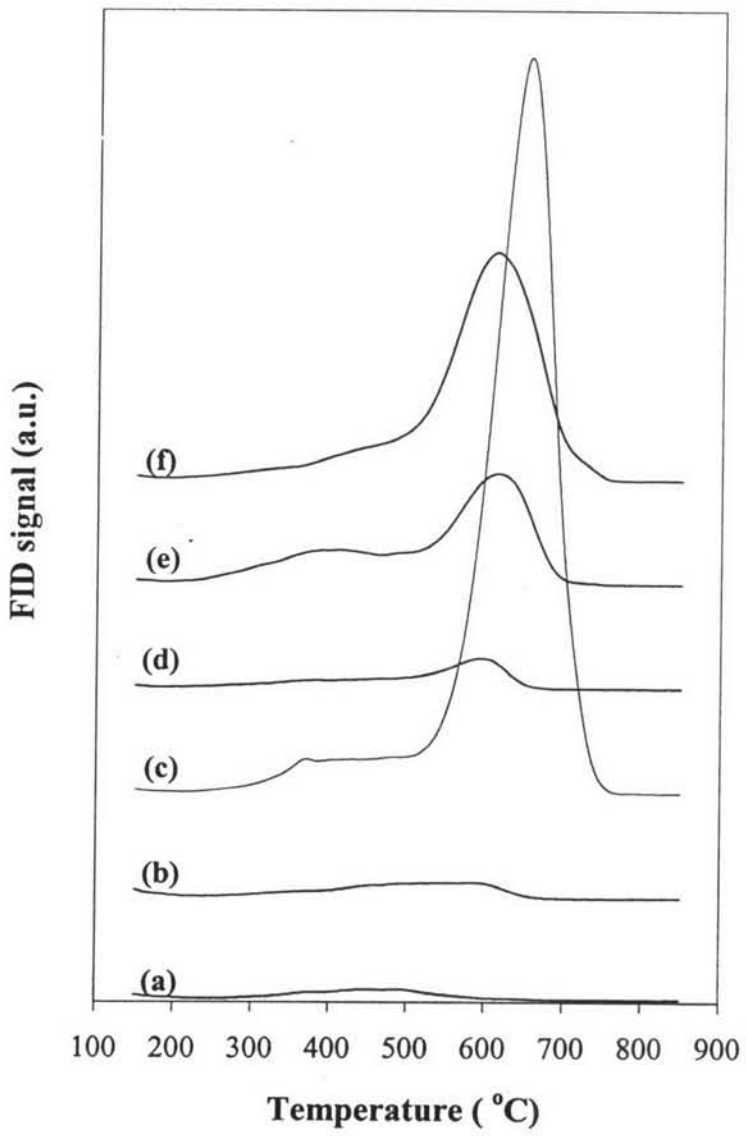

Figure 5.7 TPO profiles of spent catalysts after exposure to POX reaction at 800°C for 6 h with a heating rate of 10°C/min, an oxidizing gas containing 2% oxygen in He with a flow rate of 40 ml/min: (a) 5 wt%Ni/β"-Al_2O_3 (C/O ratio = 0.6), (b) 5 wt%Ni/β"-Al_2O_3 (C/O ratio = 1.0), (c) 5 wt%Ni/β"-Al_2O_3 (C/O ratio = 1.6), (d) 5 wt%Ni/$Ce_{0.75}Zr_{0.25}O_2$ (C/O ratio = 0.6), (e) 5 wt%Ni/$Ce_{0.75}Zr_{0.25}O_2$ (C/O ratio = 1.0), (f) 5 wt%Ni/$Ce_{0.75}Zr_{0.25}O_2$ (C/O ratio = 1.6).

5.4.3.2 The effect of water

After prolonged operation of the catalyst at 800°C with C/O ratio of unity for 6 h, both catalysts maintained their initial activities as shown in Figures 5.8 and 5.9. This indicates that our catalysts are stable for POX. However, a small amount of carbon deposition was observed for the catalysts. It has been reported that the addition of water into the feed stream of POX could reduce the amount of carbon deposition (Seo *et al.*, 2002). This led us to scrutinize such a water effect on our catalysts by introducing some steam into the POX system operating in autothermal reforming (ATR) mode.

The effect of water was studied at a C/O feed ratio of unity and H_2O/C ratio of 3:1. The activities of *iso*-octane POX in the presence of steam in the feed stream over Ni/β"-Al_2O_3 and Ni/$Ce_{0.75}Zr_{0.25}O_2$ catalysts are shown in Figures 5.10 and 5.11, respectively. By comparing the results of POX without/ with steam in the feed stream, at a given temperature, one can observe a decrease in *iso*-octane conversion for both catalysts as steam was introduced. This suggested that steam could retard the POX reaction. However, a decrease in CO selectivity but an increase in H_2 selectivity was observed resulting in obtaining higher H_2/CO ratios of 3 – 4 as compared with those obtained from POX. It is postulated that a water-gas shift reaction would play a role such a change. Interestingly, small amounts of C_2H_4, C_2H_6 and C_3H_6 were observed in the product stream at temperatures above 650°C for the 5 wt% Ni/$Ce_{0.75}Zr_{0.25}O_2$ catalyst (see Figure 5.11) whilst those were not observed in the case of POX. C_2H_6 and C_3H_6 formation is believed to be due to the thermal cracking reactions.

As seen in Figure 5.12 and 5.13, at 800°C, the *iso*-octane conversion as a function of time on stream of both catalysts remained unchanged under POX in the presence of steam. It should be noted that the Ni/$Ce_{0.75}Zr_{0.25}O_2$ catalyst yielded the complete both *iso*-octane and oxygen conversions with almost unchanged H_2 selectivity. This suggested that the Ni/$Ce_{0.75}Zr_{0.25}O_2$ catalyst is more stable than the Ni/β"-Al_2O_3 catalyst in the presence of steam. Since carbon formation was not observed for both the spent Ni/β"-Al_2O_3 and Ni/$Ce_{0.75}Zr_{0.25}O_2$ catalysts at 800°C after 6 h on stream in this study, therefore, it is conceivable that the decrease

in H_2 selectivity of the Ni/β"-Al_2O_3 catalyst might be due to phase transformation of β"-Al_2O_3 when steam was introduced to the POX system as proposed by Garbarczyk *et al.* (1983).

Figure 5.14 shows XRD patterns of fresh Ni/β"-Al_2O_3 catalyst compared with those of spent Ni/β"-Al_2O_3 catalysts from POX with and without steam in feed at 800°C. A split of the (104) plane reflection at 21.12° (2θ) indicates a phase transformation for the spent Ni/β"-Al_2O_3 catalyst obtained from POX with steam in the feed stream whereas no such split of a plane reflection was observed for the fresh Ni/β"-Al_2O_3 catalyst and the spent Ni/β"-Al_2O_3 catalyst from POX without steam.

5.5 Conclusions

It can be concluded that Ni/$Ce_{0.75}Zr_{0.25}O_2$ catalyst is more active than Ni/β"-Al_2O_3 catalyst for POX of *iso*-octane. Under POX reaction conditions, synthesis gas was produced at temperatures above 550°C on the Ni/$Ce_{0.75}Zr_{0.25}O_2$ catalyst whereas Ni/β"-Al_2O_3 required temperatures above 650°C. Alkanes and olefins (CH_4, C_2's, C_3's and C_4's) were produced over the Ni/β"-Al_2O_3 catalyst, however only CH_4 was formed over the Ni/$Ce_{0.75}Zr_{0.25}O_2$ catalyst. This suggests that Ni/β"-Al_2O_3 may be used for the simultaneous production of H_2 for fuel cells and of value-added chemicals. Both catalysts are quite stable when operated under normal conditions, yet the Ni/$Ce_{0.75}Zr_{0.25}O_2$ catalyst is more stable when rich conditions are applied. The addition of steam promotes a water-gas shift reaction resulting in a larger amount of hydrogen production and less amount of coke formation. Althogh the *iso*-octane conversion of both catalysts remains unchanged under ATR conditions but H_2 selectivity from ATR over Ni/β"-Al_2O_3 catalyst significantly decreased due to the phase change of β"-Al_2O_3 support.

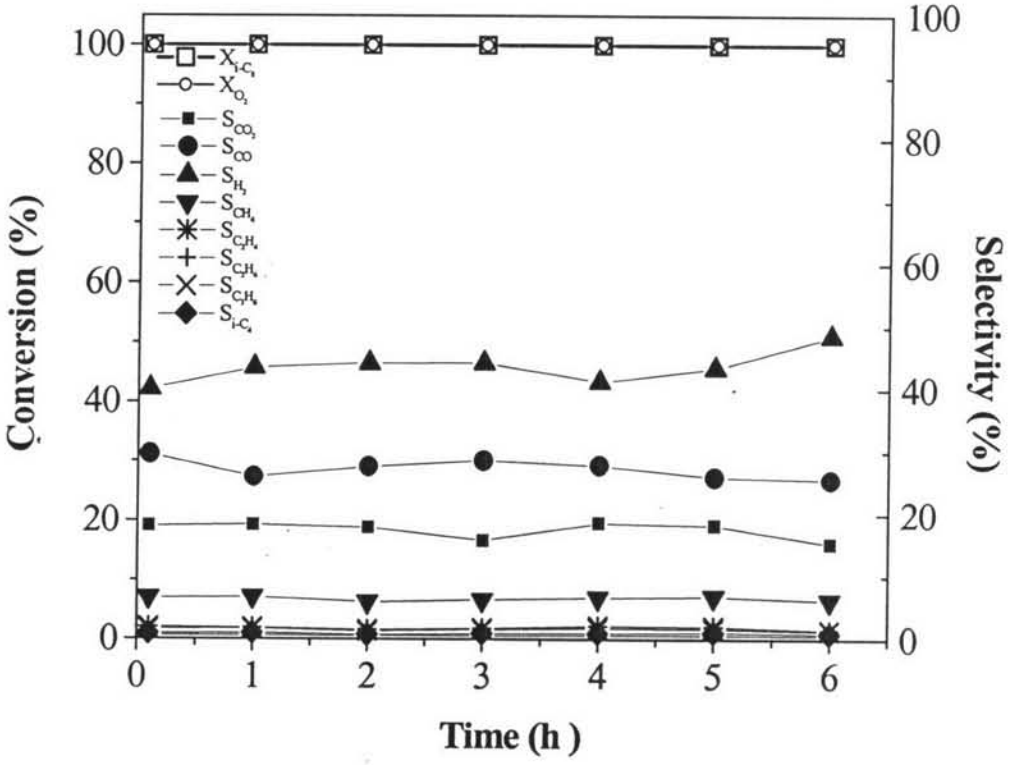

Figure 5.8 *iso*-Octane conversion, oxygen consumption (hollow symbols) and product selectivities (solid symbols) as functions of time for partial oxidation reaction over 5 wt% Ni/β"-Al_2O_3 catalyst at the temperature of 800°C with the conditions of space velocity = 80,000 h^{-1} and C/O feed molar ratio = 1.

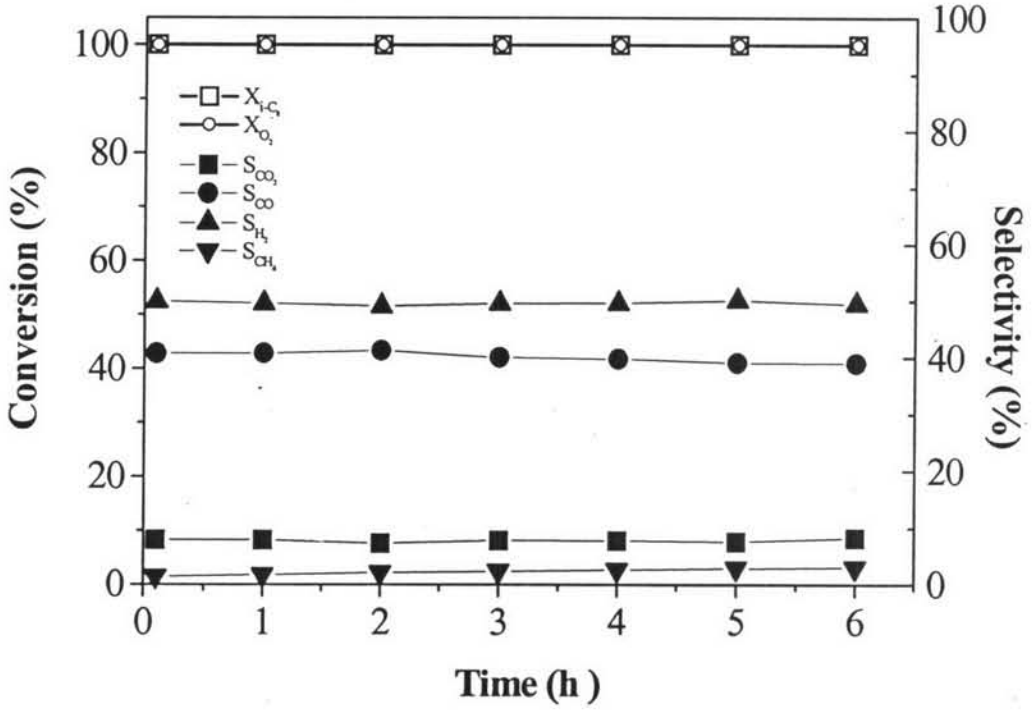

Figure 5.9 *iso*-Octane conversion, oxygen consumption (hollow symbols) and product selectivities (solid symbols) as functions of time for partial oxidation reaction over 5 wt% $Ni/Ce_{0.75}Zr_{0.25}O_2$ catalyst at the temperature of 800°C with the conditions of space velocity = 80,000 h^{-1} and C/O feed molar ratio = 1.

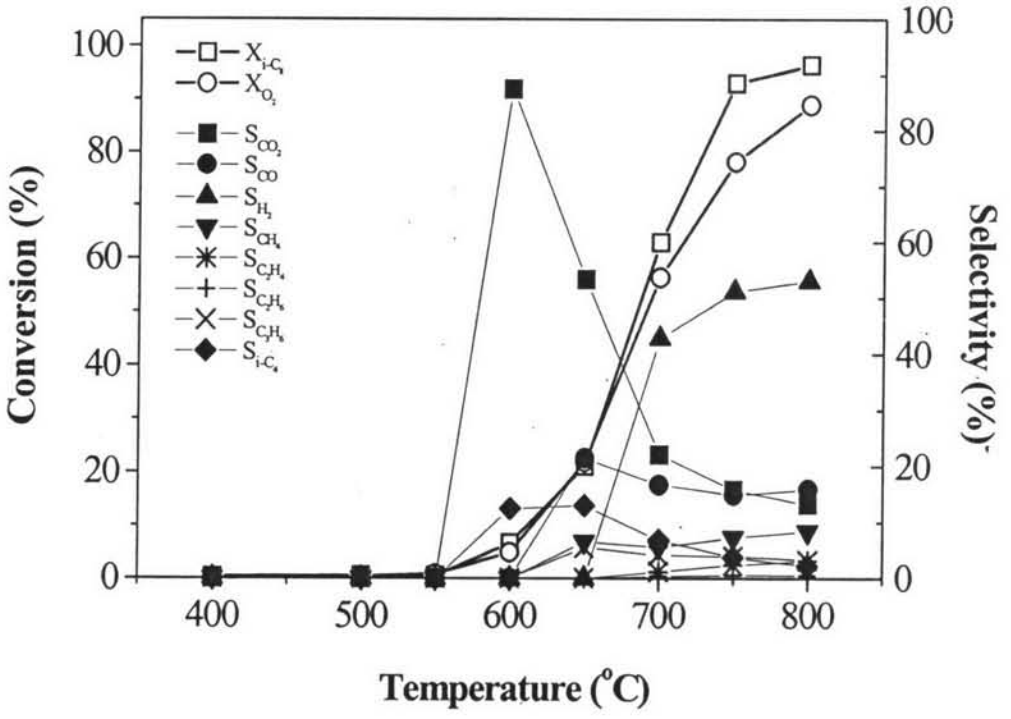

Figure 5.10 *iso*-Octane conversion, oxygen consumption (hollow symbols) and product selectivities (solid symbols) at different temperatures for POX with steam in feed over 5 wt% Ni/β"-Al_2O_3 catalyst at the conditions of space velocity = 80,000 h^{-1} and C/O feed molar ratio = 1, H_2O/C ratio = 3.

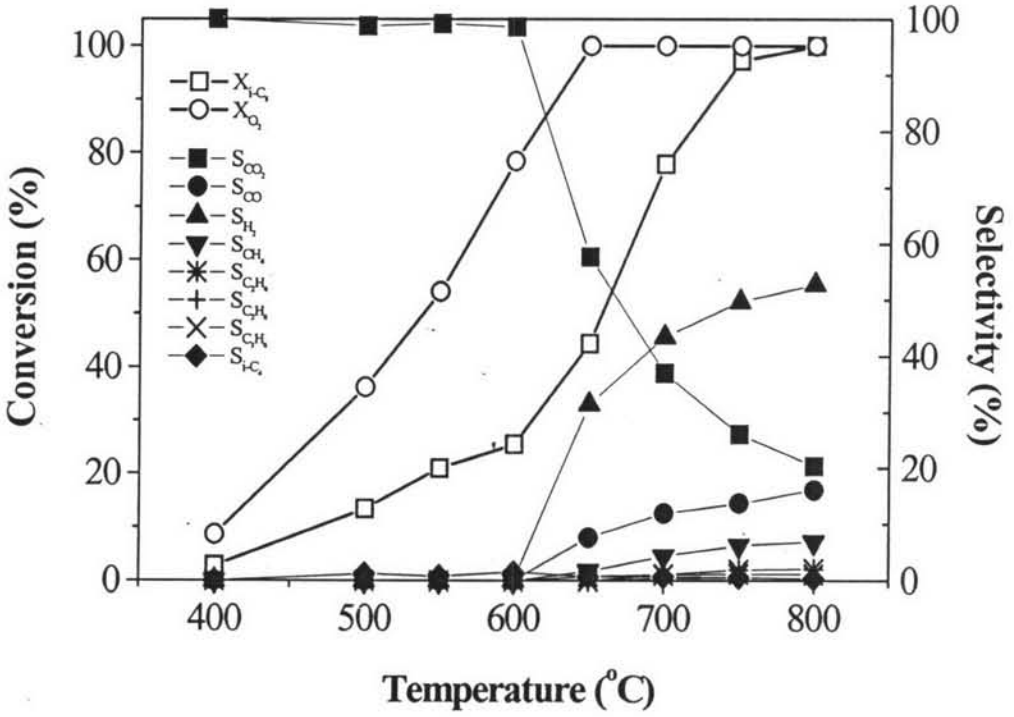

Figure 5.11 *iso*-Octane conversion, oxygen consumption (hollow symbols) and product selectivities (solid symbols) at different temperatures for POX with steam in feed over 5 wt% $Ni/Ce_{0.75}Zr_{0.25}O_2$ catalyst at the conditions of space velocity = 80,000 h^{-1} and C/O feed molar ratio = 1, H_2O/C ratio = 3.

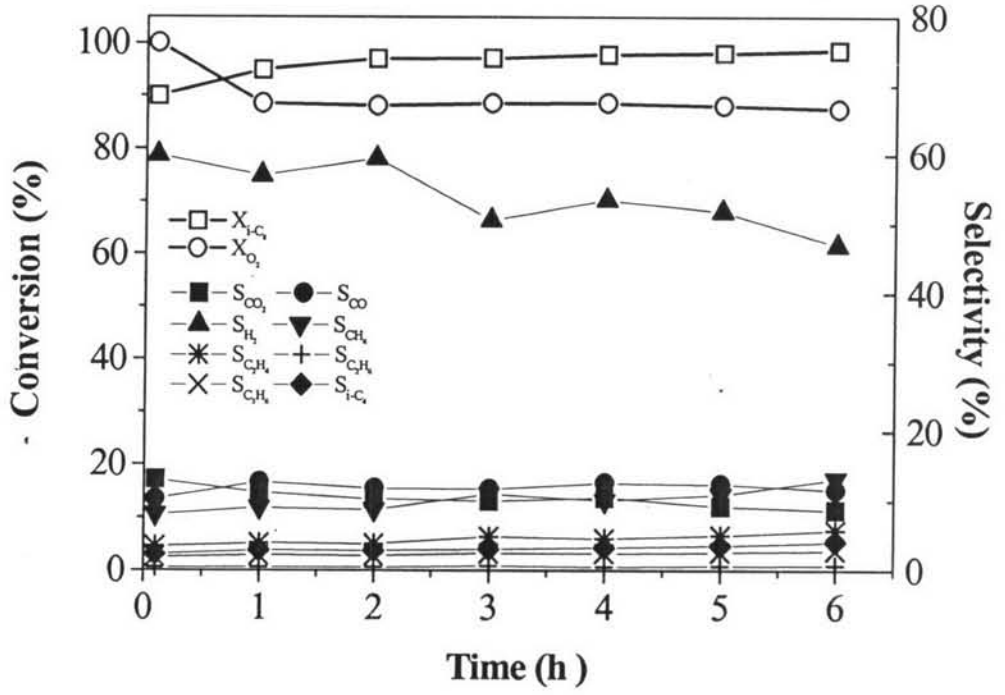

Figure 5.12 *iso*-Octane conversion, oxygen consumption (hollow symbols) and product selectivities (solid symbols) as functions of time for POX with steam in feed over 5 wt% Ni/β"-Al_2O_3 catalyst at the temperature of 800°C with the conditions of space velocity = 80,000 h^{-1} and C/O feed molar ratio = 1, H_2O/C ratio = 3.

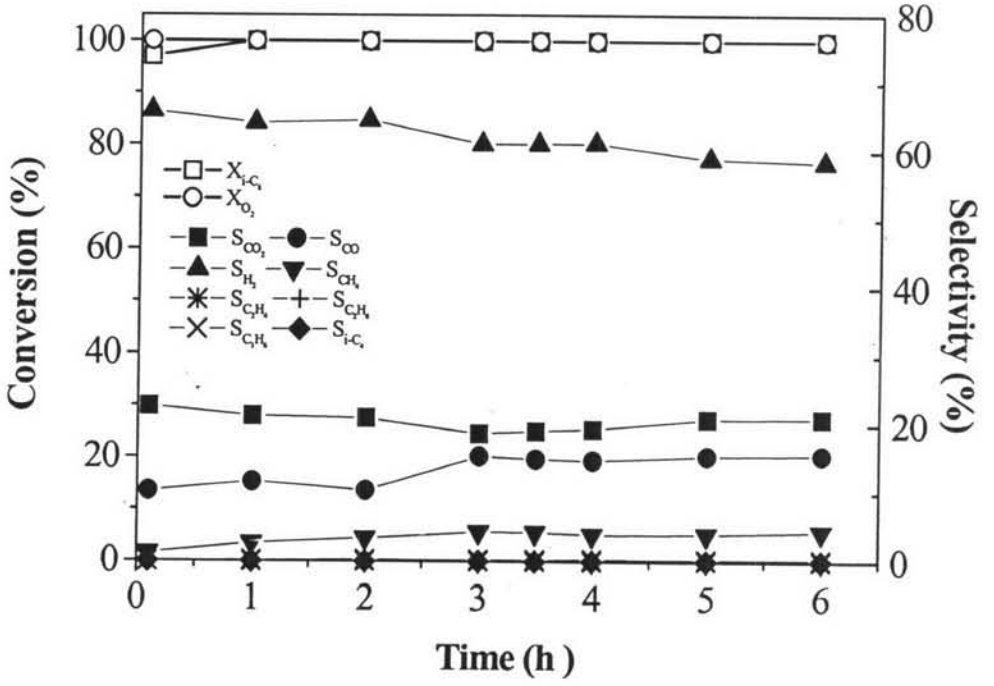

Figure 5.13 *iso*-Octane conversion, oxygen consumption (hollow symbols) and product selectivities (solid symbols) as functions of time for POX with steam in feed over 5 wt% $Ni/Ce_{0.75}Zr_{0.25}O$ catalyst at the temperature of 800°C with the conditions of space velocity = 80,000 h^{-1} and C/O feed molar ratio = 1, H_2O/C ratio = 3.

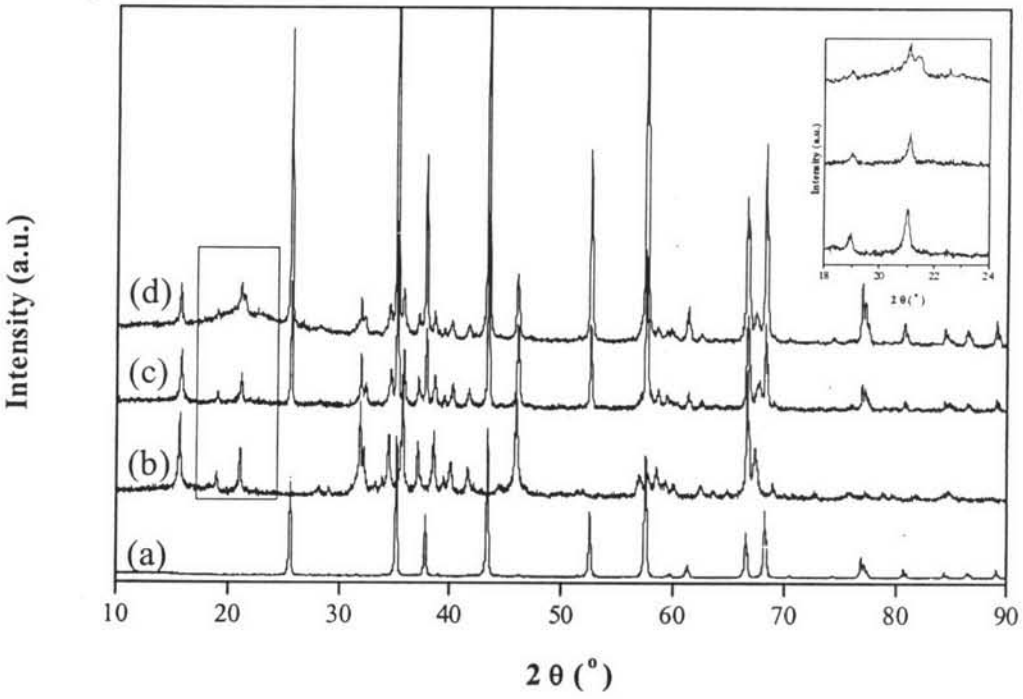

Figure 5.14 XRD patterns of α-Al_2O_3 (a), fresh 5 wt% Ni/β"-Al_2O_3 catalyst calcined at 500°C (b), spent 5 wt% Ni/β"-Al_2O_3 catalyst from partial oxidation at 800°C (c) and spent 5 wt% Ni/β"-Al_2O_3 catalyst from autothermal reaction at 800°C (d).

5.6 Acknowledgments

The authors would like to thank RGJ, Ph.D. program, Thailand Research Fund and Ratchadapiseksomphote Endowment of Chulalongkorn University for the financial support.

5.7 References

Agrawal, R.C., Gupta, R.K. (1999) Superionic Solids: Composite Electrolyte Phase-an Overview. Journal of Materials Science, 34, 1131.

Ahmed, S., and Krumpelt, M. (2001) Hydrogen from Hydrocarbon Fuels for Fuel Cells. International Journal of Hydrogen Energy, 26, 291.

Avci, K.A., Onsan, Z.I., and Trimm D.L. (2001) On-board Fuel Conversion for Hydrogen Fuel Cells: Comparison of Different Fuels by Computer Simulations. Applied Catalysis A: General, 216, 243.

Dietz III, A.G., Carlsson, A.F., Schmidt, L.D. (1996) Partial Oxidation of C_5 and C_6 Alkanes over Monolith Catalysts at Short Contact Times. Journal of Catalysis, 176, 459.

Garbarczyk, J., Jakubowski, W., Wasiucionek, M. (1983) Effect of Selected Mobile Ions on Moisture Uptake by beta"-Alumina. Solid State Ionics, 9&10, 249.

Guillet, N., Rives, A., Lalauze, R., Pijolat, C. (2003) Study of Adsorption of Oxygen on β-Al_2O_3 + Au and β-Al_2O_3 + Pt: Work Function Measurements—Proposition of a Model. Applied Surface Science, 210, 286.

Harkness, I.R., Hardacre, C., Lambert, R.M., Yentekakis, I.V., Vayenas, C.G. (1996) Ethylene Oxidation over Platinum: *In Situ* Electrochemically Controlled Promotion Using Na-β" Alumina and Studies with a Pt(111)/Na Model Catalyt. Journal of Catalysis, 160, 19.

Huff, M., Schmidt, L.D. (1995) Oxidative Dehydrogenation of Isobutane over Monoliths at Short Contact times. Journal of Catalysis, 155, 82.

Kiwi, J., Thampi, K.R., Gratzel, M. (1991) Methane Dimerization through Ion Conductors (β-Al_2O_3). Solid State Ionics, 48, 123.

Krummenacher, J.J., West, K.N., Schmidt, L.D. (2003) Catalytic Partial Oxidation of Higher Hydrocarbons at Millisecond Contact Times: Decane, Hexadecane, and Diesel Fuel. Journal of Catalysis, 215, 332.

Ming, Q., Healey, T., Allen, L., Irving, P. (2002) Steam Reforming of Hydrocarbon Fuels. Catalysis Today, 77, 51.

Moon, D.J., Sreekumar, K., Lee, S.D., Lee, B.G., Kim, H.S. (2001) Studies on Gasoline Fuel Processor System for Fuel-Cell Powered vehicles Application. Applied Catalysis A: General, 215, 1.

Montoya, J.A., Romero-Pascual, E., Gimon, C., Del Angle, P., Monzon, A., (2000) Methane Reforming with CO_2 over Ni/ZrO_2-CeO_2 Catalysts Prepared by Sol-Gel. Catalysis Today, 63, 71.

O'Connor, R.P., Klein, E.J., Schmidt, L.D. (2000) High Yields of Synthesis Gas by Millisecond Partial Oxidation of Higher Hydrocarbons. Catalysis Letters, 70, 99.

Pacheco, M., Sira, J., Kopasz, J. (2003) Reaction Kinetics and Reactor Modeling for Fuel Processing of Liquid Hydrocarbons to Produce Hydrogen: Isooctane Reforming. Applied Catalysis A: General, 250, 161.

Pengpanich, S., Meeyoo, V., Rirksomboon, T., and Bunyakiat, K. (2002) Catalytic Oxidation of Methane over CeO_2-ZrO_2 Mixed Oxide Solid Solution Catalysts Prepared via Urea Hydrolysis. Applied Catalysis A: General, 234, 221.

Pengpanich, S., Meeyoo, V., Rirksomboon, T. (2004) Methane Partial Oxidation over Ni/CeO_2-ZrO_2 mixed Oxide Solid Solution Catalysts. Catalysis Today, 93-95, 95.

Peppley, B.A., Amphlett, J.C., Kearns, L.M., and Mann, R.F. (1999) Methanol-Steam Reforming on $Cu/ZnO/Al_2O_3$. Applied Catalysis A: General, 179, 21.

Praharso, A., Adesina, A., Trimm, D.L., and Cant, N.W., (2003) Partial Oxidation of *iso*-Octane over Rh based Catalysts. Korean Journal of Chemical Engineering, 20, 468.

Roh. H., Jun, K., Dong, W., Chang, J., Park, S., and Joe, Y. (2002) Highly Active and Stable Ni/Ce-ZrO_2 Catalyst for H_2 Production from Methane. Journal of Molecular Catalysis A: Chemical, 181, 137.

Savage P.E. (2000) Mechanisms and Kinetics Models for Hydrocarbon Pyrolysis. Journal of Analytical and Applied Pyrolysis, 54, 109.

Seo, Y.S., Shirley, A., Kolaczkowski, S.T. Evaluation of Thermodynamically Favourable Operating Conditions for Production of Hydrogen in Three Different Reforming Technologies. Journal of Power Sources, 108, 213.